Dalton Transactions

ROYAL SOCIETY OF CHEMISTRY

FRONTIER

View Article Online
View Journal | View Issue

Cite this: *Dalton Trans.*, 2024, **53**, 11644

Electrocatalytic formate and alcohol oxidation by hydride transfer at first-row transition metal complexes

Navar M. White and Kate M. Waldie *

The electrocatalytic oxidation of carbon-based liquid fuels, such as formic acid and alcohols, has important applications for our renewable energy transition. Molecular electrocatalysts based on transition metal complexes provide the opportunity to explore the interplay between precise catalyst design and electrocatalytic activity. Recent advances have seen the development of first-row transition metal electrocatalysts for these transformations that operate *via* hydride transfer between the substrate and catalyst. In this Frontier article, we present the key contributions to this field and discuss the proposed mechanisms for each case. These studies also reveal the remaining challenges for formate and alcohol oxidation with first-row transition metal systems, for which we provide perspectives on future directions for next-generation electrocatalyst design.

Received 21st December 2023,
Accepted 12th June 2024

DOI: 10.1039/d3dt04304e

rsc.li/dalton

Introduction

To reduce our reliance on fossil fuels while meeting our ever-increasing global energy demand, the use of electrochemical technologies to facilitate the interconversion of renewably-derived electricity, chemicals, and usable energy is a central strategy.[1] In this regard, electrochemical oxidation of formate and alcohols is of great interest: (1) Direct formic acid or alcohol fuel cells for electricity generation.[2–6] While significant attention has been placed on H_2 fuel, liquid carbon fuels derived from CO_2 or biomass resources offer several advantages, including higher volumetric energy densities, easier storage and transportation, and compatibility with established infrastructure.[7,8] The direct use of formic acid or alcohol fuels is complementary to their indirect use as H_2 carriers for onboard H_2 delivery,[9,10] although fugitive H_2 emissions are mitigated by the direct approach.[11] (2) Alternative anode reactions for cathodic fuel production.[12–15] The electrochemical production of chemical fuels is traditionally paired with the

Department of Chemistry and Chemical Biology, Rutgers, The State University of New Jersey, 123 Bevier Road, Piscataway, New Jersey 08854, USA.
E-mail: kate.waldie@rutgers.edu

Navar M. White

Navar Mercer White received his B.A. in Chemistry with a Minor in Geometrical Mathematics from Vassar College in 2015. Mercer is currently pursuing his Ph.D. in Chemistry at Rutgers, The State University of New Jersey (New Brunswick) under the guidance of Prof. Kate M. Waldie. His current research focuses on the development of organometallic catalysts for electrocatalytic transformations and their application for sustainable chemical synthesis and renewable energy conversion.

Kate M. Waldie

Kate M. Waldie received her Ph.D. in Chemistry from Stanford University in 2016 under the guidance of Prof. Robert M. Waymouth. She completed her postdoctoral research with Professor Clifford P. Kubiak at the University of California San Diego. She is currently Assistant Professor in the Department of Chemistry and Chemical Biology at Rutgers, The State University of New Jersey (New Brunswick), where her group focuses on the design and study of molecular transition metal complexes for renewable energy storage & conversion and organic synthesis.

anodic oxygen evolution reaction (OER), which requires a large overpotential. Instead, OER may be replaced by formate or alcohol oxidation that can be accessed at less positive potentials, improving the efficacy of fuel production cells. This prospect is particularly attractive for the co-production of fuels with value-added alcohol oxidation products.[16] (3) Alcohol oxidation for fine chemical synthesis, where traditional stoichiometric chemical oxidants or hydrogen acceptors are replaced by electrochemical oxidation at the anode.[17–19]

The direct oxidation of formate or alcohols at the electrode is typically associated with high overpotentials to promote single-electron transfer (SET).[20] Thus, electrocatalysis is key to enabling substrate oxidation at milder potentials. With homogeneous transition metal complexes, investigations into electrocatalytic alcohol oxidation initially focused on metal–oxo complexes, which are strong oxidants and promote C–H oxidation *via* proton coupled electron transfer (PCET)[21–31] but require very positive potentials for regeneration of the metal–oxo. In the past two decades, transition metal electrocatalysts for alcohol and formate oxidation have been developed that operate *via* a metal-hydride intermediate, offering non-oxo-based strategies for electro-oxidation and opening the door to a wider possibility of electrocatalyst structures.[7,32–34] The metal-hydride intermediate may be formed *via* hydride transfer from the substrate, after which the starting complex must be regenerated *via* oxidation at the electrode to establish an electrocatalytic cycle (Scheme 1). Herein, we highlight the recent developments in formate and alcohol electro-oxidation *via* hydride transfer using homogeneous first-row transition metal complexes. Through these reports, we discuss the key challenges that remain in this emerging field and provide our perspective on possible strategies for future electrocatalyst development.

Thermodynamic hydricity

For catalysts that operate *via* hydride transfer (or net hydride transfer), the thermodynamic hydricity ΔG_{H^-} of the substrate and metal-hydride is a valuable consideration (Scheme 2). The hydricity of formate has been reported in water and acetonitrile: $\Delta G^\circ_{H^-} = 24.1$ and 44 kcal mol^{-1}, respectively.[35] While some aqueous hydricity measurements for metal-hydride complexes have been disclosed, a larger dataset is available in acetonitrile,[35,36] which has the additional advantage of being a common electrochemical solvent.[37] Thus, to favor formate oxidation *via* hydride transfer to a metal center, $\Delta G^\circ_{H^-}(M-H)$ of the resulting metal-hydride must be greater than 44 kcal mol^{-1}. We note that the favorability of metal–formate adduct formation and hydride transfer from this species may be relevant in certain cases.

The thermodynamic hydricity of alcohols in acetonitrile is not well established. Estimated values for 2-propanol and 2-propoxide have been obtained from computational methods (Scheme 2): protonated acetone is the product of hydride loss from 2-propanol, and acetone is analogously obtained from 2-propoxide.[38] In combination with the estimated pK_a of protonated acetone (*ca.* 0.6),[39] the former can be used to obtain an estimate for the thermodynamic potential $E^\circ_{acetone/iPrOH}$ in acetonitrile (0.19 V *vs.* $Fc^{+/0}$, the ferrocene/ferrocenium couple), which is in reasonable agreement with the value obtained using the gas-phase free energy for acetone hydrogenation (0.08 V *vs.* $Fc^{+/0}$).[40,41] As noted above, substrate coordination (alcohol or alkoxide) may be considered as well, or alcohol oxidation may proceed by a bifunctional outer-sphere mechanism involving concerted hydride and proton transfers.[42–44]

Electrocatalytic formate oxidation

Despite its relevance to renewable energy conversion, exploration of molecular transition metal complexes for electrocatalytic formate oxidation has been limited.[45–49] The first report came in 2011 based on the first-row transition metal nickel, as opposed to a noble metal center.[45] Given the hydricity of formate (*vide supra*), the authors reasoned that Ni(II)

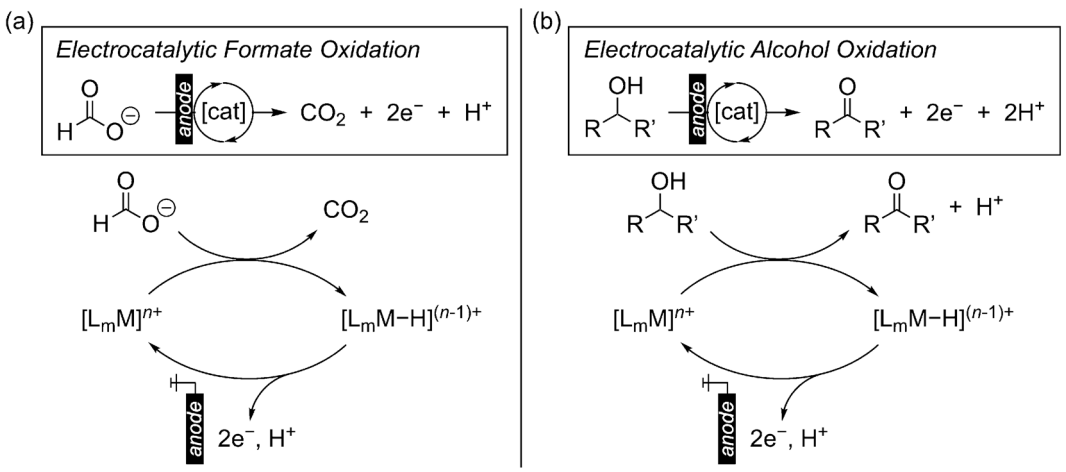

Scheme 1 General scheme for electro-oxidation of (a) formate, or (b) alcohols *via* a metal-hydride intermediate.

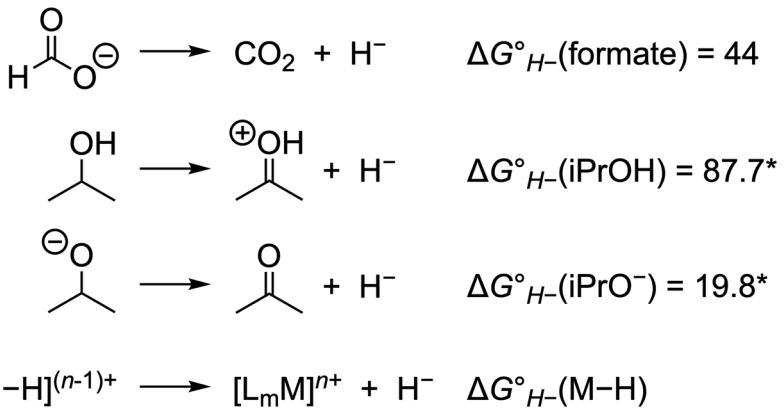

Scheme 2 Thermodynamic hydricity values (kcal mol^{-1}) in acetonitrile.[35,38] *Estimated using computational methods.[38]

complexes with two P_2N_2 ligands were likely to serve as hydride acceptors from formate based on the bidirectional reactivity of these systems with H_2.[50,51] Indeed, the hydricity of the Ni(II)-hydride analogues for **1a–1h** (Fig. 1) was measured to be greater than that of formate, ranging from $\Delta G^{\circ}_{H^-} = 55 - 64$ kcal mol^{-1}.[35,45,52]

Treatment of the Ni–P_2N_2 complexes with 1 eq. formate led to Ni(II)-hydride formation by NMR, implying that hydride transfer is accessible. Cyclic voltammetry (CV) studies revealed electrocatalytic current near the Ni(I/II) couple (Fig. 2a), and CO_2 production was confirmed in near-quantitative faradaic efficiency.[45,46] The electrocatalytic TOF was found to depend on the P_2N_2 substituents, with the fastest electrocatalyst **1a** having the least electron-rich phosphine (R = Ph) and the most basic amine (R′ = Me). Notably, the TOF was greater at smaller overpotentials η (Fig. 2b), counter to typical scaling relationships.[53] In addition, because the potential of the Ni(I/II) couple and the hydricity of the corresponding Ni(II)-hydrides are correlated, faster catalysis was achieved using the most hydridic complex.[45,52] However, other trends can similarly be constructed correlating TOF to the pendent amine basicity, making it difficult to draw conclusions about the mechanism from this data alone.

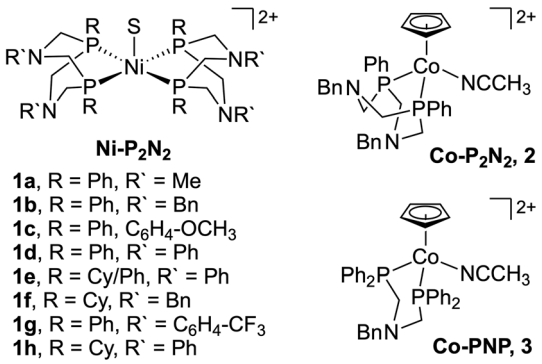

Fig. 1 Ni and Co complexes investigated for electrocatalytic formate oxidation. S = acetonitrile.

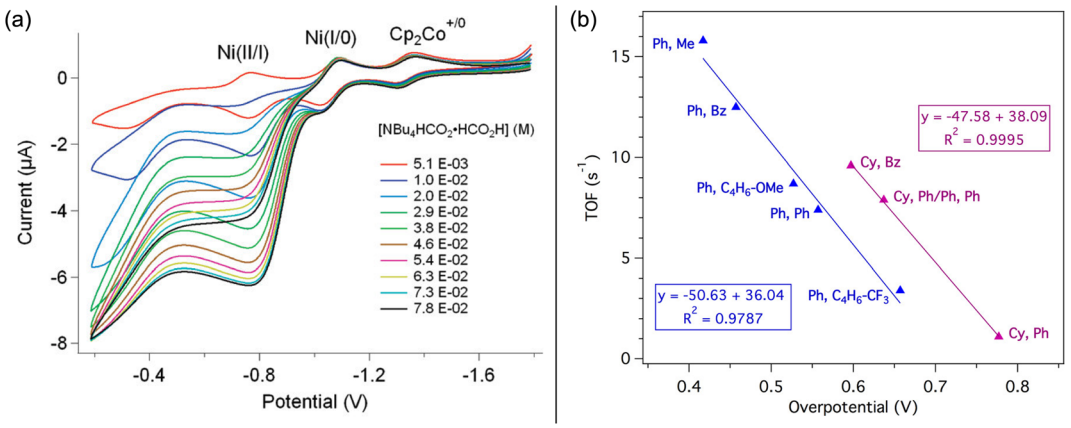

Fig. 2 (a) CVs of **1e** in benzonitrile showing electrocatalytic formate oxidation. Adapted with permission from ref. 45. Copyright 2011 American Chemical Society. (b) Correlation between TOF and overpotential for electrocatalytic formate oxidation with **1a–1h**. Data labels indicate the $P^{R}_2N^{R'}_2$ R and R′ substituents, respectively. Adapted with permission from ref. 52. Copyright 2018 American Chemical Society.

The correlation between TOF and amine basicity led the authors to propose formate oxidation by rate-limiting β-deprotonation of a Ni-formate by the pendent amine (Scheme 3, red).[45,46] A subsequent study by Xue and Ahlquist used DFT-computational methods to probe accessible pathways for this transformation.[54] Their results found that the barrier to β-deprotonation is significant and would lead to CO production, not CO_2. Instead, the calculated lowest-energy pathway is direct hydride transfer from formate and intramolecular deprotonation of the resulting Ni(II)-hydride (Scheme 3, blue). The computed barriers for these steps are similar and depend on the ligand structure and are also likely influenced by the reaction conditions. While further work is needed to better elucidate the mechanism, the pendent amines are clearly crucial. Addition of formate to [Ni(depe)$_2$] (depe = 1,2-bis(diethylphosphino)ethane) yielded the Ni(II)-hydride by CV,[45] demonstrating stoichiometric formate oxidation ($\Delta G^{\circ}_{H^-}(\mathrm{Ni-H}) = 55.3$ kcal mol^{-1})[35,55,56] but electrocatalytic turnover was not observed. Despite the remaining questions, this story is an excellent demonstration of using thermodynamic analysis to guide electrocatalyst design, while also underscoring the importance of ligand functionality for achieving rapid reactivity.

Beyond the Ni–P_2N_2 systems, two noble metal catalysts (Ir and Pt) have been reported for electrocatalytic formate oxidation.[47,48] In addition, we recently disclosed the electrocatalytic activity of Co–P_2N_2 **2** and Co–PNP **3** for formate oxidation (Fig. 1).[57] The hydricity of the corresponding Co(III)-hydrides was determined to be $\Delta G^{\circ}_{H^-} = 68.5$ and 72.3 kcal mol^{-1}, respectively, indicating that **2** and **3** are thermodynamically primed for hydride transfer from formate. Indeed, by chronoamperometry, electrocatalytic current was observed for **3** near the Co(II/III) potential in the presence of formate. Controlled-potential electrolysis (CPE) confirmed quantitative faradaic efficiency for CO_2 production.

Formate oxidation is initiated by formation of a Co(III)-formate intermediate, observable by ^{1}H NMR. Rate-limiting hydride transfer to cobalt then occurs, followed by deprotonation of the Co(III)-hydride and re-oxidation at the electrode. Interestingly, **3** exhibited a faster TOF than **2**, which may be related to different hydrogen bonding interactions between the pendent amines and biformate buffer. Further studies to probe these effects are ongoing in our group. While **2** and **3** are less active than the Ni–P_2N_2 systems, the overpotentials are comparable (*ca.* 0.5 V) and all complexes operate using formate as the base. Complexes **2** and **3** represent the second class of first-row transition metal-hydride systems for formate oxidation, encouraging more studies to explore this reactivity at first-row metals including cobalt.

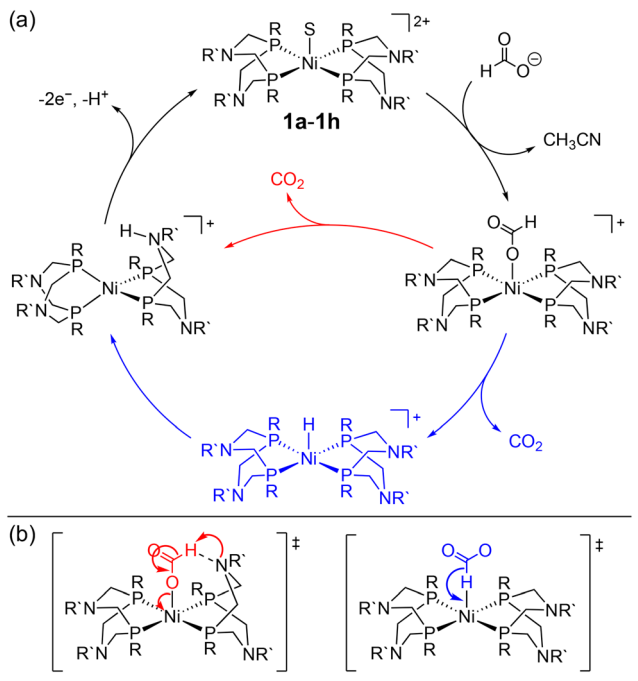

Scheme 3 (a) Proposed mechanisms for formate oxidation by **1a–1h**. (b) Proposed transition states *via* β-deprotonation (red, left) or direct hydride transfer (blue, right).[45,46,54]

Electrocatalytic alcohol oxidation

The first example of electrocatalytic alcohol oxidation by a first-row transition metal complex was reported by Appel and co-workers.[58,59] Inspired by the ability of pendent amine ligands to facilitate intramolecular proton shuttling,[60] the authors selected the Ni–P_2N_2 framework (Fig. 3) – very similar to the above structures for formate oxidation.[45,46] In their initial study, a series of Ni–P_2N_2 complexes were evaluated for chemical alcohol oxidation using triethylamine and decamethylferrocenium.[58] Complex **4c** showed the highest initial TOF for diphenylmethanol oxidation (TOF = 114 ± 5.2 h^{-1}), while the absence of pendent amine in **5a** or the presence of two P_2N_2 ligands in **1b** and **1f** led to poor activity. The latter

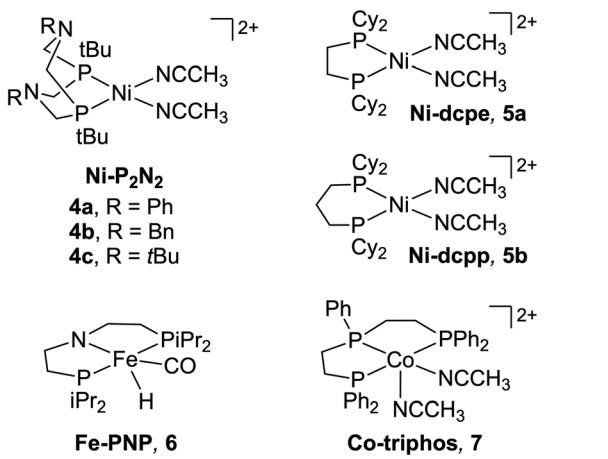

Fig. 3 Ni, Fe, and Co complexes investigated for electrocatalytic alcohol oxidation.

may be due to greater steric hindrance at the metal, disfavoring alcohol binding.

Appel and co-workers later demonstrated that **4c** is a competent electrocatalyst for alcohol oxidation.[59] As shown in Fig. 4a, electrocatalytic current was observed at $E_{cat/2}$ = −0.75 V *vs.* $Fc^{+/0}$ in the presence of benzyl alcohol and triethylamine (30 eq.; TOF = 2.5 s^{-1}). Selective formation of benzaldehyde was observed (≥90% faradaic efficiency). This landmark study was a significant step for the field of homogeneous electrocatalysis and showed the viability of first-row transition metal-hydrides for electrocatalytic alcohol oxidation. In addition, this study further expanded the electrocatalytic reactivity of Ni–P_2N_2 complexes, which had already been shown for H_2 evolution, H_2 oxidation, O_2 reduction, and of course formate oxidation.[60]

The pendent amines in the P_2N_2 ligand are crucial for electrocatalytic turnover with **4c** – this was probed in greater detail by Hall, Wiedner, and co-workers, focusing on benzyl alcohol.[61] Here, a new control complex **5b** was evaluated for which the Ni(I/II) redox potential was better matched with **4c** ($\Delta E_{1/2}$ = 30 mV) compared to **5a** ($\Delta E_{1/2}$ = 200 mV). CV studies of **5b** with benzyl alcohol and base did not show catalytic current; however, by NMR, **4c** and **5b** showed comparable rates of stoichiometric alcohol oxidation – the pendent amine is not needed for this process! Instead, the P_2N_2 ligand is thought to lower the potential for Ni-hydride oxidation *via* PCET (Fig. 4b), enabling electrocatalytic turnover at mild potentials with **4c** (η = 0.39 V).[40] This conclusion illuminates how ligand-promoted PCET may serve as a general strategy for improving the efficiency of metal-hydride catalysis.[62–64] Similar effects are likely operative for formate oxidation with the Ni-bis(phosphine) analogues **1a–1h** (*vide supra*).

Computational studies led to a more detailed picture of alcohol oxidation at **4c**.[61] Formation of the Ni-alkoxide is rate-limiting, which undergoes β-hydride elimination (Scheme 4a). The authors suggested that the P_2N_2 ligand may direct alcohol coordination *via* hydrogen bonding, but this interaction does not lower the overall barrier to Ni-alkoxide formation and deprotonation of the Ni–alcohol by the pendent amine is not accessible. These conclusions further corroborated their experimental results showing that the P_2N_2 is not necessary for rapid, stoichiometric alcohol oxidation (*vide supra*). The authors also identified an off-cycle Ni(II)–alcohol species **8**, from which deprotonation is uphill and inhibits catalytic turnover (Scheme 4b). Ligand dissociation from **8** is required to access the Ni(II)-alkoxide. Clearly, speciation of this catalyst is complicated by the accessibility of multiple coordination sites and geometries. This poses a challenge for alcohol oxidation

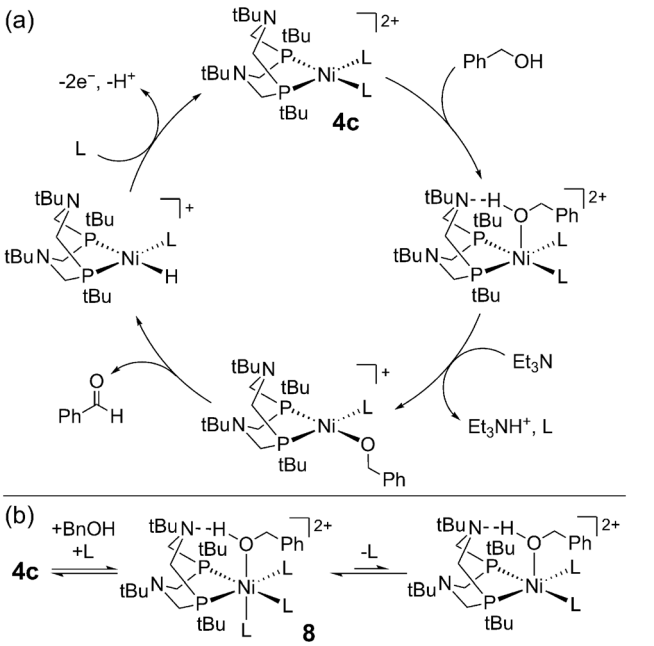

Scheme 4 (a) Proposed mechanism for benzyl alcohol oxidation by **4c**. (b) Formation of an off-cycle high-spin intermediate **8**. L = acetonitrile, triethylamine.[61]

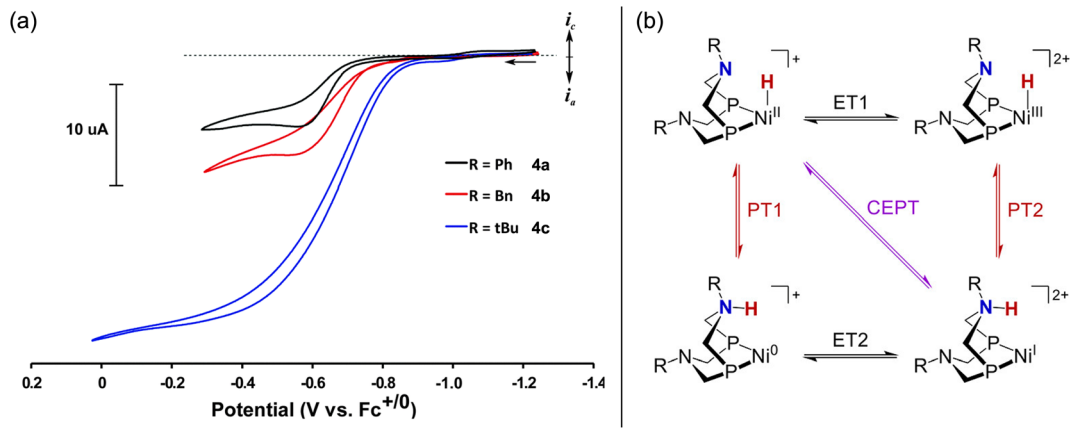

Fig. 4 (a) CVs of **4a–4c** in acetonitrile showing electrocatalytic oxidation of benzyl alcohol in the presence of triethylamine. Adapted from ref. 59 with permission from the Royal Society of Chemistry. (b) Possible PCET pathways for Ni(P_2N_2)-hydride oxidation. Adapted with permission from ref. 61. Copyright 2022 American Chemical Society.

in the presence of other coordinating species, but, as the authors point out, knowledge of this off-cycle pathway lays the groundwork for future design strategies.

In 2020, Waymouth and co-workers reported the first Fe-hydride system for alcohol oxidation.[65] Complex **6** and related compounds were previously shown to catalyze various hydrogen transfer reactions, including alcohol acceptorless dehydrogenation with impressive activity (TON ≥ 10 000) at elevated temperatures.[66–72] The ligand amide group was proposed to be directly involved in alcohol oxidation *via* a bifunctional mechanism, where hydride and proton transfer from the substrate yields **9** (Fig. 5a).[73,74] The authors[65] underscored the anticipated similarities between acceptorless dehydrogenation and alcohol electro-dehydrogenation where the same bifunctional process could be followed by either H_2 release or oxidation of the metal-hydride, respectively, reminiscent of their earlier work on the electrocatalytic activity of transfer hydrogenation catalysts.[75,76]

Complex **6** exhibited an electrocatalytic current by CV at $E_{cat/2}$ = −0.8 V *vs.* $Fc^{+/0}$ in tetrahydrofuran with 2-propanol and phosphazene base (η = 1.1 V).[40] The electrocatalytic TOF was estimated to be 1.7 s^{-1}, and CPE studies showed quantitative faradaic efficiency for acetone. The authors showed that treatment of **9** with potassium *t*-butoxide and decamethylferrocenium led to the formation of **6**, implying an overall $2e^-/2H^+$ process for the oxidation of **9** under basic conditions. DFT calculations suggested an *ECEC* pathway for this oxidation, as shown in Fig. 5b. Experimentally, very strong bases are required for electrocatalytic turnover, although the relevant computed pK_a values suggest weaker bases should promote the oxidative deprotonation of **9**. Under electrocatalytic conditions, the lifetime of this catalyst is poor (TON = 1.9), perhaps due to formation of inert Fe(0) species.[69] Nonetheless, this work established that acceptorless dehydrogenation catalysts can operate in an electrocatalytic regime, opening the door to the electrochemical evaluation of many other chemical catalysts.[77–79]

More recently, Hammes-Schiffer, Appel, and co-workers reported the electro-oxidation of benzyl alcohol using cobalt complex **7**, which features a linear triphos ligand that lacks any proton-active sites.[80] The authors posited that Co(II)-hydrides with phosphine ligands may be compatible with an alcohol oxidation scheme due to their mild potentials for oxidation and facile deprotonation of the resulting Co(III)-hydride.[81,82] Electrocatalytic current with **7** in the presence of *N*,*N*-diisopropylethylamine was not observed on the CV timescale (TOF < 0.1 s^{-1}); however, CPE conducted near the Co(I/II) couple revealed electrocatalytic production of benzaldehyde (97% faradaic efficiency, η = *ca.* 0.2 V).[40] While the TON = 19.9 for **7** was greater than for **4c** or **6**, catalyst decomposition was still significant, with 90% decomposition during electrolysis.

The proposed mechanism is initiated by substrate coordination to **7** followed by intermolecular alcohol deprotonation, β-hydride elimination to the Co(II)-hydride, and oxidative deprotonation by an *ECE* pathway to regenerate **7** (Scheme 5a). A notable aspect of this system is the absence of pendent acid/base sites on the triphos ligand. Recalling the proposed mechanism for **4c**, the pendent amines were not essential for stoichiometric alcohol oxidation and in fact did not increase the rate of this process.[61] However, the electrocatalytic activity of **4c** was dependent on oxidation of the Ni(II)-hydride *via* PCET enabled by the P_2N_2 ligand. For complex **7**, $1e^-$ oxidation of the Co(II)-hydride is facile and occurs at a more negative potential than Co(I/II) oxidation, indicating that pendent basic sites are not required for electrocatalysis. Nonetheless, it would be interesting to examine whether introduction of pendent bases into this architecture could enable Co(III)-hydride oxidation by a PCET pathway (Scheme 5b), analogous to the Ni–P_2N_2 systems. Such PCET reactivity would circumvent the original Co(I) intermediate and may shift the potential for oxidation of the Co(III)-hydride to a more negative value.

Key challenges and future outlook

Reports of first-row transition metal-hydride complexes for formate and alcohol oxidation of are limited; nonetheless, these examples offer valuable insights into some of the remaining challenges to guide future research. Key performance metrics for these systems are summarized in Table 1, with comparison to select noble metal-hydride systems for both reactions.

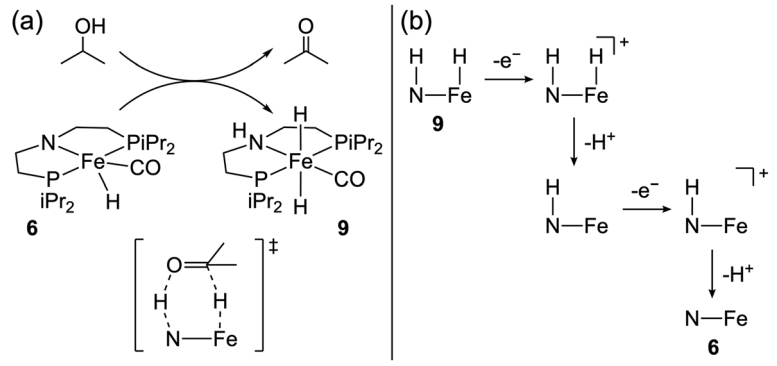

Fig. 5 (a) Proposed bifunctional pathway for 2-propanol oxidation with **6**. (b) *ECEC* oxidative deprotonation of **9**.[65]

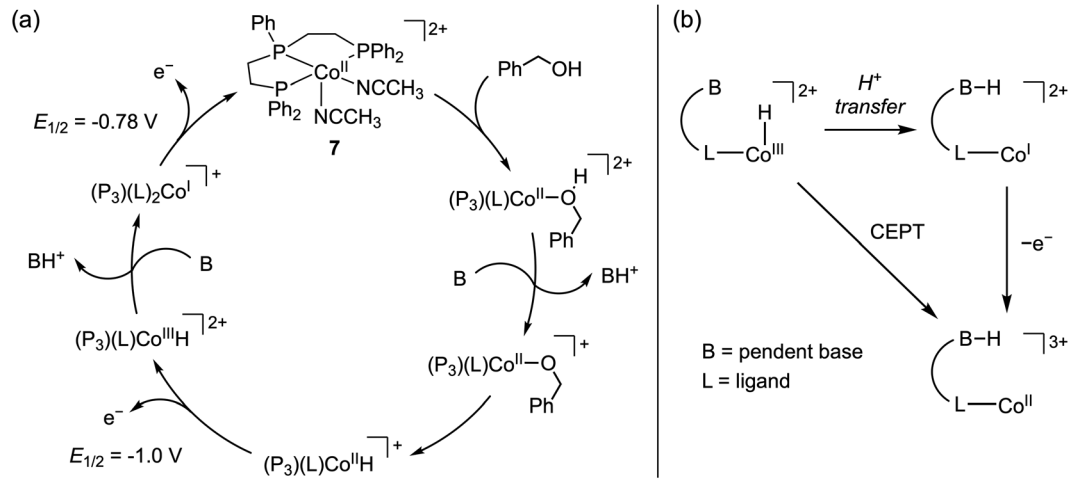

Scheme 5 (a) Proposed mechanism for benzyl alcohol oxidation by **7** with iPr_2EtN.[80] (b) Possible ligand-promoted concerted electron–proton transfer (CEPT) pathway for Co(III)-hydride oxidation.

Table 1 Summary of first-row metal-hydride electrocatalysts and select noble metal systems

Catalyst	Substrate	TOF (s^{-1})	TON	η (V)	FE (%)
1a[45]	Formate	15.8	>8	0.42[52]	93 ± 5[a]
2[57]	Formate	<0.001	>3.8	0.45	99 ± 3
3[57]	Formate	0.04	>10.7	0.57	96 ± 3
[Ir(PONOP)(H)$_3$][47]	Formate	4.8	n.d.	1.25[b]	87 ± 5
[Pt(depe)]$^{2+}$ (ref. 48)	Formate	<0.5	>2.4	0.010	90
4c[59]	Benzyl alcohol	2.5	3.1	0.39[40]	≥90
6[65]	2-Propanol	1.7	1.9	1.1[40]	100 ± 15
7[80]	Benzyl alcohol	<0.1	19.9	∼0.2[40]	97
[Ru(CNN)(dppb)H][76]	2-Propanol	4.8	>4.6	1.6[40]	94 ± 5
[Ru(NNP)(CO)ClH][33]	Ethanol	n.d.	21[c]	n.d.	62[c]
[Ir(PNP)(H)$_2$][83]	2-Propanol	n.d.	>4.0	1.5[40]	78

[a] For complex **1c**. [b] Estimated using $E^{\circ}_{CO2/formate}$ from ref. 36. [c] For the 4e$^-$ oxidation to acetate and ethyl acetate.

A general mechanism for formate and alcohol oxidation involves metal-hydride formation *via* hydride transfer and electrochemical catalyst regeneration (Scheme 1). The overall substrate oxidation process is rate-limiting for the first-row systems in Table 1. Here, the hydride accepting ability of the metal is a valuable metric. The thermodynamic hydricity of the formate oxidation catalysts has been reported;[45,52,57] however, values for the alcohol oxidation catalysts are lacking. Moving forward, as more hydricity measurements are reported, structure–activity relationships can be constructed to correlate hydride transfer energetics with electrocatalyst activity. The rate of hydride transfer, quantified as kinetic hydricity, is also an important yet understudied metric. Evaluating kinetic hydricity for the stoichiometric reaction of formate and alcohols with a series of metal complexes should reveal new design principles for promoting rapid hydride transfer, including the exploration of solvent effects that can significantly impact hydride transfer rates.[84–87] In addition, the initial interaction of the substrate (hydride donor) with the metal (hydride acceptor) is proposed for these systems. Thus, increasing the metal Lewis acidity while maintaining an open coordination site is likely crucial, especially for alcohol oxidation given that substrate coordination to **4c** and **7** is unfavorable.[59,61,80] Greater Lewis acidity at the metal will also increase the acidity of the metal–alcohol intermediate. A simplistic approach may introduce more electron-withdrawing ligands, but such electronic changes will also affect other performance metrics (*vide infra*). An interesting prospect would be to explore redox-active ligands, which have been shown to enhance Lewis acidity at metal centers by serving as reversible electron reservoirs.[79,88]

The first-row examples in Table 1 largely feature pendent base ligands. Hydrogen-bonding interactions between the pendent amines and biformate may be relevant to the activity of **1–3**, but the P_2N_2 ligand in **4c** does not assist the alcohol oxidation steps. Looking to chemical dehydrogenation catalysts, many first-row systems utilize metal–ligand cooperativity (MLC) to enable rapid substrate oxidation,[77,79] as with complex **6** where proton transfer to the ligand occurs with hydride addition at the metal. Future efforts should delve deeper into MLC pathways for first-row electrocatalysis, leveraging established ligand designs. Many of these chemical catalysts not only exhibit impressive activity but also catalyst lifetimes that far exceed the electrocatalytic examples. Rigid MLC pincer ligands may be beneficial to this end, though it will be important to evaluate stability under electrochemical conditions. A key challenge will be balancing productive substrate oxidation with the pK_a requirements for electrocatalysis. As observed with **6**, ligand deprotonation requires strong bases, translating to large overpotentials. Limited pK_a measurements of such ligands have been reported,[89–91] underscoring the need for further studies to elucidate the interplay between metal and ligand thermodynamic and kinetic properties for electrocatalysis.

The introduction of pendent hydrogen-bond donors, instead of pendent bases, offers another approach to improving the kinetics of substrate oxidation by stabilizing the hydride transfer transition state.[77,79] Furthermore, pendent charged groups may deliver transition state stabilization through electrostatic interactions.[92,93] The addition of exogenous Lewis acidic cations has been shown to increase the rate of formic acid dehydrogenation with iron catalysts.[94,95] Intramolecular electrostatic effects *via* catalyst modification may provide even greater benefit.[93,96–99]

To establish an electrocatalytic cycle following substrate oxidation, $2e^-/1H^+$ oxidative deprotonation of the metal-hydride is needed (Scheme 1). Shifting the requisite potential for catalyst regeneration to more negative values is desirable, but inductive ligand modifications will decrease the Lewis acidity of the metal center, resulting in weaker substrate interactions and lower catalytic rates. Therein lies a key challenge in molecular electrocatalysis: overcoming molecular scaling relationships to achieve high kinetic activity at small overpotentials. For formate and alcohol oxidation, notable advances have been made with the Ni–P_2N_2 systems. With **1a–1h** and **4c**, the pendent amines significantly lower the potential for metal-hydride oxidation by accessing PCET pathways. The pendent amine properties can be tuned largely independent of the metal center,[60] allowing the amine basicity to be adjusted without compromising substrate activation *via* hydride transfer at the metal. This contributes to the impressive TOFs for these systems at modest overpotentials, even in comparison to noble-metal examples. However, extending this strategy to more robust complexes is still needed. Redox-active ligands and pendent charged groups, noted above as possible strategies for improving rates of substrate reactivity, may also engender different TOF-η trends by altering the correlation between the metal Lewis acidity to promote metal-hydride formation and the redox properties of the catalyst. Similar strategies have been applied for overcoming normal scaling relationships with other electrocatalytic reactions,[100] and warrant exploration in the context of formate and alcohol electro-oxidation.

The Ni–P_2N_2 systems access fast rates at modest overpotentials thanks to intramolecular PCET pathways that enable oxidation of the metal-hydride at mild potentials. Future studies may explore related intermolecular approaches using hydrogen atom transfer (HAT) mediators to promote homolytic cleavage of the metal-hydride, bypassing higher-energy intermediates from stepwise electron and proton transfer (Scheme 6).[101,102] Key to this approach is selecting HAT mediators for which hydrogen atom abstraction from the metal-hydride is favorable, and that can be electrochemically regenerated at a more negative potential than oxidation of the metal-hydride. This approach was recently demonstrated with noble-metal catalysts for alcohol oxidation.[83,103] Through careful selection of HAT mediators, the electrocatalytic overpotentials were lowered by *ca.* 0.5 V while maintaining rapid TOFs, counter to normal scaling relationships.[40] As additional thermodynamic metrics for first-row metal-hydride complexes become available, the rational selection of viable HAT mediators will become feasible – an exciting prospect for future investigations into oxidative electrocatalysis.

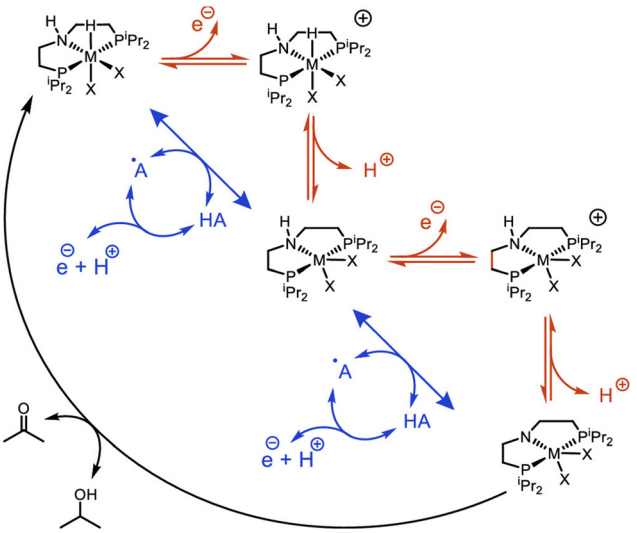

Scheme 6 Metal-hydride oxidative deprotonation by stepwise (red) or mediated (blue) pathways. Reprinted with permission from ref. 83. Copyright 2020 American Chemical Society.

While the studies highlighted here focused on catalysts involving discrete metal-hydride intermediates, alternative pathways that operate *via* net hydride transfer offer new opportunities for electrocatalyst design. Yang and co-workers posited that orthogonal hydride transfer, where the electron and proton transfer sites are not co-located as a metal-hydride, may have distinct advantages for the electrocatalytic interconversion of CO_2 and formate, inspired by formate dehydrogenase.[104] Very recently, a new iron electrocatalyst for formate oxidation was reported, for which the proposed mechanism invokes separate sites for proton and electron transfers to achieve net hydride transfer.[49] The TOF is impressive (*ca.* 10^3 s^{-1}), nearly two orders of magnitude greater than for **1a**. However, the electrocatalytic potential is very high – more than 1.1 V positive of **1–3**. It will be interesting to see whether these potentials can be shifted more negative while still accessing this orthogonal mechanism. It also remains to be seen whether alcohol oxidation may be accessible by an analogous net hydride transfer mechanism. We note the similarities to the reactivity of early metal–oxo electrocatalysts[21–31] and the copper-nitroxyl radical co-catalytic system developed by Badalyan and Stahl,[105] where net hydride abstraction is achieved in an orthogonal fashion.

An ideal electrocatalyst will operate near the standard thermodynamic potential for formate or alcohol oxidation, which depends on the solvent and solution basicity. For formate oxidation, the simplest system would utilize a formate buffer to provide the requisite basic conditions. Thus, catalyst design efforts should target electrocatalytic turnover with biformate near the defined thermodynamic potential in a particular solvent.[106] Alcohol electro-oxidation also requires basic

conditions, and thus the standard thermodynamic potential varies with base selection.[40] In this regard, the base and solvent can be viewed as additional experimental handles for minimizing the electrocatalytic overpotential. However, the solution basicity must be matched with the pK_a requirements of the catalytic mechanism, and the solvent must be compatible with the catalyst and base. Other parameters such as thermodynamic and kinetic hydricity are also solvent-dependent.[35,84–87] Thus, a holistic approach where these factors are considered in parallel is recommended toward the design of optimized electrocatalysts and reaction conditions.

Author contributions

Conceptualization, K.M.W.; writing – original draft, N.M.W. and K.M.W.; writing – review and editing, N.M.W. and K.M.W.; supervision, K.M.W.

Data availability

No primary research results, software, or code have been included and no new data were generated or analyzed as part of this review.

Conflicts of interest

There are no conflicts to declare.

Acknowledgements

This work was supported by Rutgers, The State University of New Jersey.

References

1 N. S. Lewis and D. G. Nocera, *Proc. Natl. Acad. Sci. U. S. A.*, 2006, **103**, 15729–15735.
2 M. Grasemann and G. Laurenczy, *Energy Environ. Sci.*, 2012, **5**, 8171–8181.
3 L. An and R. Chen, *J. Power Sources*, 2016, **320**, 127–139.
4 D. M. Fadzillah, S. K. Kamarudin, M. A. Zainoodin and M. S. Masdar, *Int. J. Hydrogen Energy*, 2019, **44**, 3031–3054.
5 S. S. Siwal, S. Thakur, Q. B. Zhang and V. K. Thakur, *Mater. Today Adv.*, 2019, **14**, 100182.
6 A. Q. K. Nguyen, H. Q. Pham, S. T. M. Huynh and T. T. Huynh, *Adv. Sustainable Syst.*, 2023, **7**, 2300205.
7 A. W. Cook and K. M. Waldie, *ACS Appl. Energy Mater.*, 2020, **3**, 38–46.
8 S. Esquivel-Elizondo, A. H. Mejia, T. Sun, E. Shrestha, S. P. Hamburg and I. B. Ocko, *Front. Energy Res.*, 2024, **11**, 1207208.
9 V. Yadav, G. Sivakumar, V. Gupta and E. Balaraman, *ACS Catal.*, 2021, **11**, 14712–14726.
10 J. Eppinger and K.-W. Huang, *ACS Energy Lett.*, 2017, **2**, 188–195.
11 I. Dutta, R. K. Parsapur, S. Chatterjee, A. M. Hengne, D. Tan, K. Peramaiah, T. I. Solling, O. J. Nielson and K.-W. Huang, *ACS Energy Lett.*, 2023, **8**, 3251–3257.
12 D. Wang, P. Wang, S. Wang, Y.-H. Chen, H. Zhang and A. Lei, *Nat. Commun.*, 2019, **10**, 2796.
13 M. T. Bender, X. Yuan and K.-S. Choi, *Nat. Commun.*, 2020, **11**, 4594.
14 S. Verma, S. Lu and P. J. A. Kenis, *Nat. Energy*, 2019, **4**, 466–474.
15 J. Na, B. Seo, K. J. C. W. Lee, H. Lee, Y. J. Hwang, B. K. Min, D. K. Lee, H.-S. Oh and U. Lee, *Nat. Commun.*, 2019, **10**, 5193.
16 Y. Pan, H. Zhang, B. Zhang, F. Gong, J. Feng, H. Huang, S. Vanka, R. Fan, Q. Cao, M. Shen, Z. Li, Z. Zou, R. Xiao and S. Chu, *Nat. Commun.*, 2023, **14**, 1013.
17 B. A. Frontana-Uribe, R. D. Little, J. G. Ibanez, A. Palma and R. Vasquez-Medrano, *Green Chem.*, 2010, **12**, 2099–2119.
18 E. J. Horn, B. R. Rosen and P. S. Baran, *ACS Cent. Sci.*, 2016, **2**, 302–308.
19 M. Yan, Y. Kawamata and P. S. Baran, *Chem. Rev.*, 2017, **117**, 13230–13319.
20 F. Wang and S. S. Stahl, *Acc. Chem. Res.*, 2020, **53**, 561–574.
21 M. S. Thompson and T. J. Meyer, *J. Am. Chem. Soc.*, 1982, **104**, 4106–4115.
22 L. Roecker and T. J. Meyer, *J. Am. Chem. Soc.*, 1987, **109**, 746–754.
23 W. K. Seok and T. J. Meyer, *J. Am. Chem. Soc.*, 1988, **110**, 7358–7367.
24 C.-M. Che, C. Ho and T.-C. Lau, *J. Chem. Soc., Dalton Trans.*, 1991, 1901–1907.
25 C.-K. Li, W.-T. Tang, C.-M. Che, K.-Y. Wong, R.-J. Wang and T. C. W. Mak, *J. Chem. Soc., Dalton Trans.*, 1991, 1909–1914.
26 Y.-K. Lai and K.-Y. Wong, *Electrochim. Acta*, 1993, **38**, 1015–1021.
27 A. Gerli, J. Reedijk, M. T. Lakin and A. L. Speks, *Inorg. Chem.*, 1995, **34**, 1836–1843.
28 V. J. Catalano, R. A. Heck, C. E. Immoos, A. Öhman and M. G. Hill, *Inorg. Chem.*, 1998, **37**, 2150–2157.
29 M. Rodriguez, I. Romero, A. Llobet, A. Deronzier, M. Biner, T. Parella and H. Stoeckli-Evans, *Inorg. Chem.*, 2001, **40**, 4150–4156.
30 A. Paul, J. F. Hull, M. R. Norris, Z. Chen, D. H. Ess, J. J. Concepcion and T. J. Meyer, *Inorg. Chem.*, 2011, **50**, 1167–1169.
31 A. K. Vannucci, J. F. Hull, Z. Chen, R. A. Binstead, J. J. Concepcion and T. J. Meyer, *J. Am. Chem. Soc.*, 2012, **134**, 3972–3975.
32 M. Trincado, J. Bösken and H. Grützmacher, *Coord. Chem. Rev.*, 2021, **443**, 213967.

33 N. von Wolff, O. Rivalda-Wheelaghan and D. Tocqueville, *ChemElectroChem*, 2021, **8**, 4019–4027.
34 I. Fokin, K.-T. Kuessner and I. Siewert, *Synthesis*, 2022, **54**, 295–314.
35 E. S. Wiedner, M. B. Chambers, C. L. Pitman, R. M. Bullock, A. J. M. Miller and A. M. Appel, *Chem. Rev.*, 2016, **116**, 8655–8692.
36 K. M. Waldie, A. L. Ostericher, M. H. Reineke, A. F. Sasayama and C. P. Kubiak, *ACS Catal.*, 2018, **8**, 1313–1324.
37 S. Katipamula, N. M. White and K. M. Waldie, *Chem. Catal.*, 2023, **3**, 100561.
38 J. T. Muckerman, P. Achord, C. Creutz, D. E. Polyansky and E. Fujita, *Proc. Natl. Acad. Sci. U. S. A.*, 2012, **109**, 15657–15662.
39 I. Fokin and I. Siewert, *Chem. – Eur. J.*, 2020, **26**, 14137–14143.
40 A. L. Speelman, J. B. Gerken, S. P. Heins, E. S. Wiedner, S. S. Stahl and A. M. Appel, *Energy Environ. Sci.*, 2022, **15**, 4015–4024.
41 *CRC Handbook of Chemistry and Physics*, 81st Edition, ed. D. R. Lide, CRC Press, Boca Raton, FL, 2000.
42 R. Noyori, M. Yamakawa and S. Hashiguchi, *J. Org. Chem.*, 2001, **66**, 7931–7944.
43 P. A. Dub and J. C. Gordon, *ACS Catal.*, 2017, **7**, 6635–6655.
44 P. Chakraborty, S. Pradhan and B. Sundararaji, in *Topics in Organometallic Chemistry*, Springer, Berlin, Heidelberg, 2023.
45 B. R. Galan, J. Schöffel, J. C. Linehan, C. Seu, A. M. Appel, J. A. S. Roberts, M. L. Helm, U. J. Kilgore, J. Y. Yang, D. L. DuBois and C. P. Kubiak, *J. Am. Chem. Soc.*, 2011, **133**, 12767–12779.
46 C. Seu, A. M. Appel, M. D. Doud, D. L. DuBois and C. P. Kubiak, *Energy Environ. Sci.*, 2012, **5**, 6480–6490.
47 J. Bi, P. Hou and P. Kang, *ChemCatChem*, 2019, **11**, 2069–2072.
48 D. W. Cunningham, J. M. Barlow, R. S. Velazquez and J. Y. Yang, *Angew. Chem., Int. Ed.*, 2020, **59**, 4443–4447.
49 Y. Li, J.-Y. Chen, X. Zhang, Z. Peng, Q. Miao, W. Chen, F. Xie, R.-Z. Liao, S. Ye, C.-H. Tung and W. Wang, *J. Am. Chem. Soc.*, 2023, **145**, 26915–26924.
50 A. D. Wilson, R. H. Newell, M. J. McNevin, J. T. Muckerman, M. R. DuBois and D. L. DuBois, *J. Am. Chem. Soc.*, 2005, **128**, 358–366.
51 M. Rakowski DuBois and D. L. DuBois, *Chem. Soc. Rev.*, 2009, **38**, 62–72.
52 K. M. Waldie, F. M. Brunner and C. P. Kubiak, *ACS Sustainable Chem. Eng.*, 2018, **6**, 6841–6848.
53 M. L. Pegis, C. F. Wise, B. Koronkiewicz and J. M. Mayer, *J. Am. Chem. Soc.*, 2017, **139**, 11000–11003.
54 L. Xue and M. S. G. Ahlquist, *Inorg. Chem.*, 2014, **53**, 3281–3289.
55 D. E. Berning, B. C. Noll and D. L. DuBois, *J. Am. Chem. Soc.*, 1999, **121**, 11432–11447.
56 J. C. Calvin, M. Alex, W. W. Ellis and L. D. Daniel, *J. Am. Chem. Soc.*, 2002, **124**, 1918–1925.
57 S. Katipamula, A. W. Cook, I. Niedzwiecki, T. J. Emge and K. M. Waldie, *ChemRxiv*, 2023, DOI: **10.26434/chemrxiv-2023-tfn6t**.
58 C. J. Weiss, P. Das, D. L. Miller, M. L. Helm and A. M. Appel, *ACS Catal.*, 2014, **4**, 2951–2958.
59 C. J. Weiss, E. S. Wiedner, J. A. S. Roberts and A. M. Appel, *Chem. Commun.*, 2015, **51**, 6172–6174.
60 E. S. Wiedner, A. M. Appel, S. Raugei, W. J. Shaw and R. M. Bullock, *Chem. Rev.*, 2022, **122**, 12427–12474.
61 T. Gunasekara, Y. Tong, A. L. Speelman, J. D. Erickson, A. M. Appel, M. B. Hall and E. S. Wiedner, *ACS Catal.*, 2022, **12**, 2729–2740.
62 C. J. Curtis, A. Miedaner, R. Ciancanelli, W. W. Ellis, B. C. Noll, M. Rakowski DuBois and D. L. DuBois, *Inorg. Chem.*, 2003, **42**, 216–227.
63 L. E. Fernandez, S. Horvath and S. Hammes-Schiffer, *J. Phys. Chem. C*, 2012, **116**, 3171–3180.
64 S. Horvath, L. E. Fernandez, A. V. Soudackov and S. Hammes-Schiffer, *Proc. Natl. Acad. Sci. U. S. A.*, 2012, **109**, 15663–15668.
65 E. A. McLoughlin, B. D. Matson, R. Sarangi and R. Waymouth, *Inorg. Chem.*, 2020, **59**, 1453–1460.
66 P. J. Bonitatibus, Jr., S. Chakraborty, M. D. Doherty, O. Siclovan, W. D. Jones and G. L. Soloveichik, *Proc. Natl. Acad. Sci. U. S. A.*, 2015, **112**, 1687–1692.
67 E. Alberico, P. Sponholz, C. Cordes, M. Nielsen, H.-J. Drexler, W. Baumann, H. Junge and M. Beller, *Angew. Chem., Int. Ed.*, 2013, **52**, 14162–14166.
68 S. Werkmeister, K. Junge, B. Wendt, E. Alberico, H. Jiao, W. Baumann, H. Junge, F. Gallou and M. Beller, *Angew. Chem., Int. Ed.*, 2014, **53**, 8722–8726.
69 S. Chakraborty, P. O. Lagaditis, M. Förster, E. A. Bielinski, N. Hazari, M. C. Holthausen, W. D. Jones and S. Schneider, *ACS Catal.*, 2014, **4**, 3994–4003.
70 S. Chakraborty, W. W. Brennessel and W. D. Jones, *J. Am. Chem. Soc.*, 2014, **136**, 8564–8567.
71 S. Chakraborty, H. Dai, P. Bhattacharya, N. T. Fairweather, M. S. Gibson, J. A. Krause and G. Hairong, *J. Am. Chem. Soc.*, 2014, **136**, 7869–7872.
72 F. Schneck, M. Assmann, M. Balmer, K. Harms and R. Langer, *Organometallics*, 2016, **35**, 1931–1943.
73 X. Yang, *ACS Catal.*, 2013, **3**, 2684–2688.
74 H. Jiao, K. Junge, E. Alberico and M. Beller, *J. Comput. Chem.*, 2016, **37**, 168–176.
75 K. R. Brownell, C. C. L. McCrory, C. E. D. Chidsey, R. H. Perry, R. N. Zare and R. M. Waymouth, *J. Am. Chem. Soc.*, 2013, **135**, 14299–14305.
76 K. M. Waldie, K. R. Flajslik, E. A. McLoughlin, C. E. D. Chidsey and R. M. Waymouth, *J. Am. Chem. Soc.*, 2017, **139**, 738–748.
77 G. A. Filonenko, R. van Putten, E. J. M. Hensen and E. A. Pidko, *Chem. Soc. Rev.*, 2018, **47**, 1459–1483.
78 S. Budweg, K. Junge and M. Beller, *Catal. Sci. Technol.*, 2020, **10**, 3825–3842.

79 L. Alig, M. Fritz and S. Schneider, *Chem. Rev.*, 2019, **119**, 2681–2751.
80 S. P. Heins, P. E. Schneider, A. L. Speelman, S. Hammes-Schiffer and A. M. Appel, *ACS Catal.*, 2021, **11**, 6384–6389.
81 R. Ciancanelli, B. C. Noll, D. L. DuBois and M. Rakowski DuBois, *J. Am. Chem. Soc.*, 2002, **124**, 2984–2992.
82 S. C. Marinescu, J. R. Winkler and H. B. Gray, *Proc. Natl. Acad. Sci. U. S. A.*, 2012, **109**, 15127–15131.
83 C. M. Galvin and R. M. Waymouth, *J. Am. Chem. Soc.*, 2020, **142**, 19368–19378.
84 K. R. Brereton, N. E. Smith, N. Hazari and A. J. M. Miller, *Chem. Soc. Rev.*, 2020, **49**, 7929–7948.
85 S. Ilic, A. Alherz, C. B. Musgrave and K. D. Glusac, *Chem. Soc. Rev.*, 2018, **47**, 2809–2836.
86 M. R. Espinosa, M. Z. Ertem, M. Barakat, Q. J. Bruch, A. P. Deziel, M. R. Elsby, F. Hasanayn, N. Hazari, A. J. M. Miller, M. V. Pecoraro, A. M. Smith and N. E. Smith, *J. Am. Chem. Soc.*, 2022, **144**, 17939–17954.
87 M. R. Elsby, M. R. Espinosa, M. Z. Ertem, A. P. Deziel, N. Hazari, A. J. M. Miller, A. H. Paulus and M. V. Pecoraro, *Organometallics*, 2023, **42**, 3005–3012.
88 V. Lyaskovskyy and B. de Bruin, *ACS Catal.*, 2012, **2**, 270–279.
89 D. Tocqueville, F. Crisanti, J. Guerrero, E. Nubret, M. Robert, D. Milstein and N. von Wolff, *Chem. Sci.*, 2022, **13**, 13220–13224.
90 C. L. Mathis, J. Geary, Y. Ardon, M. S. Reese, M. A. Philliber, R. T. VanderLinden and C. T. Saouma, *J. Am. Chem. Soc.*, 2019, **141**, 14317–14328.
91 B. Askevold, A. Friedrich, M. R. Buchner, B. Lewall, A. C. Filippou, E. Herdtweck and S. Schneider, *J. Organomet. Chem.*, 2013, **744**, 35–40.
92 C. Costentin, S. Drouet, M. Robert and J.-M. Savéant, *Science*, 2012, **338**, 90–94.
93 I. Azcarate, C. Costentin, M. Robert and J.-M. Savéant, *J. Am. Chem. Soc.*, 2016, **138**, 16639–16644.
94 E. A. Bielinski, P. O. Lagaditis, Y. Zhang, B. Q. Mercado, C. Würtele, W. H. Bernskoetter, N. Hazari and S. Schneider, *J. Am. Chem. Soc.*, 2014, **136**, 10234–10237.
95 E. A. Bielinski, M. Förster, Y. Zhang, W. H. Bernskoetter, N. Hazari and M. C. Holthausen, *ACS Catal.*, 2015, **5**, 2404–2415.
96 D. J. Martin, B. Q. Mercado and J. M. Mayer, *Sci. Adv.*, 2020, **6**, eaaz3318.
97 R. Zhang and J. J. Warren, *J. Am. Chem. Soc.*, 2020, **142**, 13426–13434.
98 D. J. Martin and J. M. Mayer, *J. Am. Chem. Soc.*, 2021, **143**, 11423–11434.
99 N. D. Loewen, S. Pattanayak, R. Herber, J. C. Fettinger and L. A. Berben, *J. Phys. Chem. Lett.*, 2021, **12**, 3066–3073.
100 W. Nie and C. C. L. McCrory, *Dalton Trans.*, 2022, **51**, 6993–7010.
101 M. Bourrez, R. Steinmetz, S. Ott, F. Gloaguen and L. Hammarström, *Nat. Chem.*, 2015, **7**, 140–145.
102 T. Huang, E. S. Rountree, A. P. Traywick, M. Bayoumi and J. L. Dempsey, *J. Am. Chem. Soc.*, 2017, **140**, 14655–14669.
103 E. A. McLoughlin, K. C. Armstrong and R. M. Waymouth, *ACS Catal.*, 2020, **10**, 11654–11662.
104 J. Y. Yang, T. A. Kerr, X. S. Wang and J. M. Barlow, *J. Am. Chem. Soc.*, 2020, **142**, 19438–19445.
105 A. Badalyan and S. S. Stahl, *Nature*, 2016, **535**, 406–410.
106 B. M. Stratakes, J. L. Dempsey and A. J. M. Miller, *ChemElectroChem*, 2021, **8**, 4161–4180.